Journal of Biomolecular NMR, **12:** 325–332, 1998.
KLUWER/ESCOM

An HNCO-based pulse scheme for the measurement of $^{13}C^{\alpha}$–$^{1}H^{\alpha}$ one-bond dipolar couplings in ^{15}N, ^{13}C labeled proteins

Daiwen Yang[a], Joel R. Tolman[a], Natalie K. Goto[b] & Lewis E. Kay[a]
[a]*The Protein Engineering Centers of Excellence and Departments of Medical Genetics, Biochemistry and Chemistry, University of Toronto, Toronto, ON, Canada M5S 1A8;* [b]*Department of Biochemistry, University of Toronto, Toronto, ON, Canada M5S 1A8*

Received 19 February 1998; Accepted 17 March 1998

Key words: $^{13}C^{\alpha}$–$^{1}H^{\alpha}$ dipolar couplings, bicelles, HNCO

Abstract

A triple resonance pulse scheme is presented for recording $^{13}C^{\alpha}$–$^{1}H^{\alpha}$ one-bond dipolar couplings in ^{15}N, ^{13}C labeled proteins. HNCO correlation maps are generated where the carbonyl chemical shift is modulated by the $^{13}C^{\alpha}$–$^{1}H^{\alpha}$ coupling, with the two doublet components separated into individual data sets. The experiment makes use of recently described methodology whereby the protein of interest is dissolved in a dilute solution of bicelles which orient above a critical temperature, thus permitting measurement of significant couplings (Tjandra and Bax, 1997a). An application to the protein ubiquitin is described.

Macromolecular structure determination by NMR spectroscopy has long been predicated on the establishment of internuclear distance restraints via the nuclear Overhauser effect and dihedral angle restraints from measurement of scalar coupling constants (Wüthrich, 1986). More recently, the use of restraints derived from residual dipolar couplings has been introduced for the refinement of structures of proteins and protein complexes (Tjandra et al., 1997; Tolman et al., 1995). The development of methodology for the accurate and precise measurement of residual dipolar couplings in macromolecular systems is strongly motivated by their fundamentally different sensitivity to structure and dynamics compared to measured NOEs and scalar coupling constants. These dipolar couplings can, in principle, be used to establish the spatial relationship of remote segments of the molecule (Tjandra et al., 1997), as well as serving as motional probes of dynamic processes spanning the picosecond (ps) to millisecond (ms) timescales (Tolman et al., 1997).

Initial work with dipolar couplings focused on systems with alignment established by an anisotropic molecular susceptibility (Tjandra et al., 1996; Tolman et al., 1995). In the case of diamagnetic proteins the major contributions to the susceptibility anisotropy arise from peptide bond and aromatic groups and the net sum from all the contributors in a molecule is small. Thus, differences in one bond ^{15}N–NH dipolar couplings ranging from 0 to approximately -0.2 Hz were obtained for the protein ubiquitin from measurements recorded at 600 and 360 MHz (Tjandra et al., 1996). In contrast, in the case of the paramagnetic protein cyanometmyoglobin, dipolar couplings ranging from 5 to -1 Hz were measured at 750 MHz (Tolman et al., 1995), while couplings on the order of 2 Hz were measured from ^{15}N–NH splittings recorded at 750 and 360 MHz for a complex of the transcription factor GATA-1 and a 16-base-pair oligonucleotide (Tjandra et al., 1997).

Recently Tjandra and Bax described a method for significantly increasing the size of dipolar couplings in macromolecules, including systems where alignment based on the magnetic susceptibility anisotropy would lead to couplings of only a few tenths of a Hz (Tjandra and Bax, 1997a). The approach is based on dissolving the molecule of interest in a solution containing bicelles composed of a mixture (mol/mol) of approximately 1:3 dihexanoyl phosphatidylcholine (DHPC) and dimyris-

toyl phosphatidylcholine (DMPC) (Sanders et al., 1994; Sanders and Schwonek, 1992). Above a critical temperature, which is a function of the lipid concentration and the ratio of the lipid components, the bicelle particles strongly align with the magnetic field and a small residual alignment of the macromolecule results. Below the critical temperature the solvent is isotropic and, as mentioned above, for diamagnetic macromolecules the residual dipolar couplings are essentially zero. Thus, the difference in couplings measured below and above the temperature of bicelle ordering gives the residual dipolar coupling. Based on this approach Tjandra and Bax report ^{15}N–NH and $^{13}C^{\alpha}$–$^{1}H^{\alpha}$ dipolar couplings for ubiquitin as large as +15 and −40 Hz, respectively (1997a).

Although a significant amount of effort has been expended in the development of robust pulse schemes for the measurement of ^{15}N–NH dipolar couplings (Tjandra et al., 1996; Tolman and Prestegard, 1996a, 1996b), fewer experiments have been devised for the measurement of residual one-bond $^{13}C^{\alpha}$–$^{1}H^{\alpha}$ dipolar couplings. Tjandra and Bax have described a constant-time ^{13}C–^{1}H HSQC sequence which measures $^{13}C^{\alpha}$–$^{1}H^{\alpha}$ splittings using the principle of quantitative *J*-correlation (Tjandra and Bax, 1997b), but this method is limited to applications involving small proteins. With this in mind we have developed an HNCO-based sequence for recording $^{13}C^{\alpha}$–$^{1}H^{\alpha}$ dipolar couplings and demonstrate the utility of the method by an application to the protein ubiquitin.

Figure 1 illustrates the pulse scheme that has been developed for the measurement of one-bond $^{13}C^{\alpha}$–$^{1}H^{\alpha}$ dipolar couplings in ^{15}N, ^{13}C labeled proteins. The sequence is similar in many respects to previously published HNCO (Kay et al., 1990) and HNCOCA (Bax and Ikura, 1991) pulse schemes and therefore only a brief description of the experiment is provided. Magnetization transfer is described concisely according to,

$$\mathrm{NH}\xrightarrow{J_{NH}}{}^{15}\mathrm{N}\xrightarrow{J_{NC'}}{}^{13}\mathrm{C}'(t_1)\xrightarrow{J_{C'C\alpha}}{}^{13}\mathrm{C}^{\alpha}(\kappa t_1)\xrightarrow{J_{C'C\alpha}}{}^{13}\mathrm{C}'\xrightarrow{J_{NC'}}{}^{15}\mathrm{N}(t_2)\xrightarrow{J_{NH}}\mathrm{NH}(t_3), \quad (1)$$

where the active couplings involved in each transfer step are listed above the arrows, t_i ($i = 1, 2, 3$) is an acquisition time and κ a constant, typically 0.5 (see below).

The essential idea behind the experiment is to record an HNCO correlation map where the carbonyl chemical shift of residue *i* is modulated by the one-bond $^{13}C^{\alpha}$–$^{1}H^{\alpha}$ coupling of the same residue. This is accomplished through the use of two t_1 evolution periods, with the first recording chemical shift and the second coupling evolution. Recently an analogous accordion-style experiment (Bodenhausen and Ernst, 1981) has been proposed by Tolman and Prestegard for recording ^{15}N–NH couplings in proteins (Tolman and Prestegard, 1996a). Unfortunately the use of this strategy generates doublets in the carbonyl dimension, severely compromising resolution in the case of applications to larger proteins. In addition, because of the limited acquisition time which can be used for measuring the couplings in the first place (see below), the doublet components are not resolved to baseline and the measured splittings therefore underestimate the true coupling values. In order to avoid these problems, it is important that two spectra be recorded, with separation of the doublet components (one per spectrum), as described below.

The key features of the pulse scheme can be illustrated by considering a brief operator description, where only the essential terms are retained, multiplicative factors ignored and relaxation neglected. At point *a* in Figure 1, spin coherence of the form $N_zC'_z$ is present, where X_z denotes the *z* component of magnetization from spin *X*. Using the first line of the phase cycle described in the legend to the figure, the term of interest at point *b* is proportional to $N_zC'_zC^{\alpha}{}_z\cos(\omega_{C'}t_1)$, where $\omega_{C'}$ is the carbonyl resonance frequency. The subsequent period between points *b* and *c*, of duration $1/(2J_{CH})$ where J_{CH} is the one-bond $^{13}C^{\alpha}$–$^{1}H^{\alpha}$ scalar coupling, is crucial for the separate selection of each of the two doublet components. For $\phi4 = -x$, evolution due to $^{13}C^{\alpha}$–$^{1}H^{\alpha}$ coupling is refocused so that the term of interest at point *c* is the same as at *b*. During the interval extending between points *d* and *e* the cosine modulated component of magnetization is selected, so that at e the relevant signal is of the form $N_zC'_zC^{\alpha}{}_z\cos(\omega_{C'}t_1)\cos(\pi\mathbf{J}\kappa t_1)\cos(\pi J_{C\alpha\beta}\kappa t_1)$, where **J** is the sum of the one-bond $^{13}C^{\alpha}$–$^{1}H^{\alpha}$ scalar and dipolar couplings and $J_{C\alpha\beta}$ is the one-bond $^{13}C^{\alpha}$-$^{13}C^{\beta}$ coupling. Subsequently, the magnetization is transferred back to the ^{15}N and finally to the NH spins, using coherence transfer elements that have been described in detail in the literature (Muhandiram and Kay, 1994).

A second experiment is recorded where the phases $\phi2$, $\phi5$ and $\phi7$ are incremented by 90°, with inversion of the phases $\phi4$ and $\phi8$. A similar argument to that given above establishes that the signal of interest in this case is proportional to a term of the form $\sin(\omega_{C'}t_1)\sin(\pi\mathbf{J}\kappa t_1)\cos(\pi J_{C\alpha\beta}\kappa t_1)$. By recording data

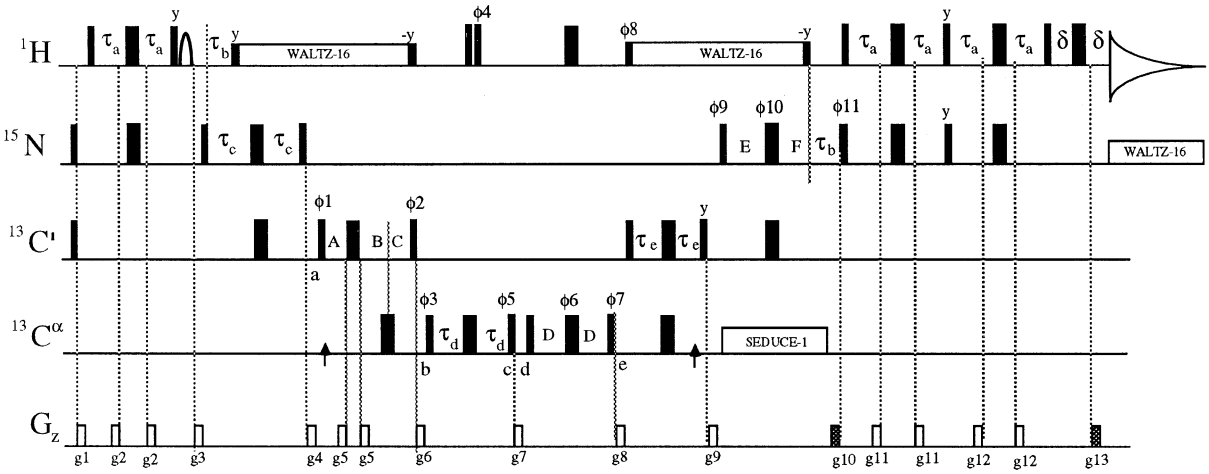

Figure 1. Pulse scheme for the measurement of $^{13}C^\alpha$–$^1H^\alpha$ one-bond dipolar couplings in ^{15}N, ^{13}C labeled proteins. All narrow (wide) pulses are applied with a flip angle of 90° (180°) and are along the *x* axis, unless indicated otherwise. The ^1H and ^{15}N carrier frequencies are centered at 4.7 (water) and 119 ppm, respectively, while the ^{13}C carrier is centered at 176 ppm except between points *b*–*e* when the carrier is at 58 ppm. All proton pulses are applied with a field of 28 kHz, with the exception of the 2 ms water selective 90° flip back pulse prior to the gradient g3, the WALTZ-decoupling elements (Shaka et al., 1983) and the flanking pulses (6 kHz). The proton pulse in the center of the period extending from *d*-*e* is of the composite variety ($90_x180_y90_x$) (Freeman et al., 1980). ^{15}N pulses are applied with a 6.3 kHz field, while decoupling during acquisition is achieved with a 1 kHz field. All $^{13}C'$ pulses have a field strength of $\Delta/\sqrt{15}$, where Δ is the separation in Hz between the centers of the $^{13}C'$ and $^{13}C^\alpha$ shifts (Kay et al., 1990). All $^{13}C^\alpha$ 90° (180°) pulses are applied at a strength of $\Delta/\sqrt{15}$ ($\Delta/\sqrt{3}$). The vertical arrows indicate the positions of the Bloch–Siegert compensation pulses (Vuister and Bax, 1992). Note that the $^{13}C^\alpha$ 180° pulse during the $2\tau_e$ period is applied prior to the $^{13}C'$ refocusing pulse. The first and last $^{13}C^\alpha$ 180° pulses are phase modulated by 118 ppm (Boyd and Scoffe, 1989; Patt, 1992). $^{13}C^\alpha$ decoupling during the ^{15}N evolution period was achieved using WALTZ-16 with the shape of each of the elements (320 μs) given by the SEDUCE-1 profile (cosine modulated by 118 ppm) (McCoy and Mueller, 1992). The delays used are: $\tau_a = 2.3$ ms; $\tau_b = 5.5$ ms; $\tau_c = 12.4$ ms; $\tau_d = 1.75$ ms; $\tau_e = 4.5$ ms; $\delta = 0.5$ ms; $A = \tau_e - n\zeta$; $B = t_1/2 - n\zeta$; $C = t_1/2 + \tau_e$; $D = \kappa t_1/2$; $E = T_N - t_2/2$; $F = T_N + t_2/2 - \tau_b$; $T_N = 12.4$ ms. A value of $\kappa = 0.5$ is used. The value of $n = 0, 1, 2, \ldots (N - 1)$, where N is the number of complex t_1 points, is incremented for each complex t_1 point and $\zeta = (\tau_e - g5)/(N - 1)$ (Grzesiek and Bax, 1993; Logan et al., 1993). The phase cycling employed for the data set in which the signal is modulated according to $\cos(\omega_{C'}t_1)\cos(\pi\mathbf{J}\kappa t_1)\cos(\pi J_{C\alpha\beta}\kappa t_1)$ is given by: ϕ1=(*x*,−*x*); ϕ2=*y*; ϕ3=(*x*,−*x*); ϕ4=−*x*; ϕ5=*x*; ϕ6=2(*x*),2(*y*),2(−*x*),2(−*y*); ϕ7=*x*; ϕ8=−*y*; ϕ9=*x*; ϕ10=4(*x*),4(−*x*); ϕ11=*x*; acq=2(*x*),2(−*x*). For the data set modulated by $\sin(\omega_{C'}t_1)\sin(\pi\mathbf{J}\kappa t_1)\cos(\pi J_{C\alpha\beta}\kappa t_1)$ the phases ϕ2, ϕ5 and ϕ7 are incremented by 90°, while ϕ4 and ϕ8 are increased by 180°. The cosine and sine modulated spectra are recorded in an interleaved manner. Quadrature detection in F_1 is achieved by States-TPPI of ϕ1 (Marion et al., 1989), while quadrature in F_2 makes used of the enhanced sensitivity pulsed field gradient method (Kay et al., 1992; Schleucher et al., 1993), where for each value of t_2 separate data sets are recorded for (*g*10,ϕ11) and (−*g*10,ϕ11+180°). For each successive t_2 value ϕ9 and the phase of the receiver are incremented by 180°. The duration and strengths of the gradients are: *g*1=(0.5 ms, 8G/cm); *g*2=(0.5 ms, 5G/cm); *g*3=(1 ms, 15G/cm); *g*4=(1.5 ms, 10G/cm); *g*5=(0.1 ms, 25G/cm); *g*6=(1 ms, 8G/cm); *g*7=(1 ms, 15G/cm); *g*8=(1.2 ms, −15G/cm); *g*9=(1 ms, 10G/cm); *g*10=(1.25 ms, −30G/cm); *g*11=(0.4 ms, 5G/cm); *g*12=(0.3 ms, 4G/cm); *g*13=(0.125 ms, 29G/cm). Decoupling is interrupted prior to the application of gradients (Kay, 1993).

from these two experiments (and their corresponding quadrature components) separately and subsequently adding and subtracting data sets in a post-acquisition manner, spectra are generated with correlations at $\omega_{C'}(i) + \pi\kappa\mathbf{J}$, $\omega_N(i+1)$, $\omega_{NH}(i+1)$ (spectrum 1) and $\omega_{C'}(i) - \pi\kappa\mathbf{J}$, $\omega_N(i+1)$, $\omega_{NH}(i+1)$ (spectrum 2). Note that the resolution in F_1 is not sufficient to observe the passive $^{13}C^\alpha$–$^{13}C^\beta$ coupling (see below). Values of the $^{13}C^\alpha$–$^1H^\alpha$ couplings are obtained directly by subtracting F_1 cross-peak positions from the two spectra since the separation is given by $\kappa\mathbf{J}$ Hz. It is noteworthy that an essentially identical method for measuring scalar couplings has been published by Yang and Nagayama (1996) and a ismilar method has been described by Sorensen and coworkers (1997).

As described above, the passive $^{13}C^\alpha$–$^{13}C^\beta$ coupling which evolves between points d and e in Figure 1 and the rapid $^{13}C^\alpha$ transverse relaxation time which is operative during this interval necessitate the use of a short κt_1 acquisition time. The $^{13}C^\alpha$–$^{13}C^\beta$ coupling is ≈ 35 Hz, while $^{13}C^\alpha$ T_2 values may be as short as 15–20 ms for proteins in the 20–30 kDa molecular weight regime (Yamazaki et al., 1994), necessitating the use of $\kappa t_{1,\max}$ values $\leq \approx 12$ ms. In contrast, in order to achieve sufficient resolution in F_1, carbonyl chemical shift evolution must proceed for a period ($t_{1,\max}$) of significantly longer duration than $\kappa t_{1,\max}$.

The value of κ must not be chosen to be too small since the measured one-bond $^{13}C^{\alpha}$–$^{1}H^{\alpha}$ coupling is κ**J** Hz and the error in the measured value of **J** and hence in the dipolar coupling is thus scaled by a factor of 1/κ. In practice we find that a value of $\kappa = 0.5$ is a good compromise between resolution, sensitivity and attenuation of the measured coupling value.

In the above discussion a uniform value for the $^{13}C^{\alpha}$–$^{1}H^{\alpha}$ coupling has been assumed. While this assumption is reasonable for molecules dissolved in an isotropic medium the situation is quite different in the case of an oriented sample. For example, couplings which deviate by as much as 30 Hz from the canonical J_{CH} value of ≈ 140 Hz (Vuister et al., 1992) have been measured in the ubiquitin/bicelle (4.5% w/v) sample employed in the present study. Therefore, the $\sin(\omega_{C'}t_1)\sin(\pi\mathbf{J}\kappa t_1)\cos(\pi J_{C\alpha\beta}\kappa t_1)$ term is reduced by a factor, $\sin(\pi\mathbf{J}2\tau_d)$, relative to the $\cos(\omega_{C'}t_1)\cos(\pi\mathbf{J}\kappa t_1)\cos(\pi J_{C\alpha\beta}\kappa t_1)$ modulated component, leading to the incomplete separation of multiplet components. Spectra are obtained where the intensity of the principle multiplet component is given by the factor $0.5[1 + \sin(\pi\mathbf{J}2\tau_d)]$, while the minor component has an intensity of $0.5[1 - \sin(\pi\mathbf{J}2\tau_d)]$. For the largest dipolar coupling measured in our sample (see below), $\sin(\pi\mathbf{J}2\tau_d) = 0.94$ and the principle component is over 30 fold larger than the minor component. Of course, for the majority of residues the relative ratio of multiplet intensities is even larger than 30 and clean separation of the components is achieved.

In order to evaluate the method a sample of 1.0 mM ^{15}N, ^{13}C labeled ubiquitin was prepared in which DHPC and DMPC were added in the ratio 1:2.9 (mol/mol) to give a net concentration of lipid of ≈ 4.5% w/v. The sample included 20 mM potassium phosphate, pH 5.8, 10% D_2O/90% H_2O. All spectra were recorded on a Varian Unity+ 500 MHz spectrometer equipped with a pulsed field gradient unit and a triple resonance probe with an actively shielded z-gradient. Experiments were performed at 35 °C and 25 °C for oriented and unoriented bicelles, respectively, and the splittings measured from data sets recorded at these two temperatures were subtracted to yield dipolar coupling values. During stability trials involving a number of different proteins we noted that the lifetimes of the samples were critically dependent on the pH and salt concentration of the solution. In general stability was improved by working at pH values close to neutral and at low salt concentrations (< 50 mM). A small amount of tetradecyltrimethylammonium bromide (T.T.A.B., ≈ 1–5 mM) was added to the bicelle samples and found to significantly increase stability (Prestegard, personal communication). Thus, the sample used in the present study contained 0.7 mM T.T.A.B.

Figure 2 presents portions of F_1–F_3 planes showing cross-peaks from residues Ala 28, Pro 19 and Phe 4 of ubiquitin obtained from a data set collected with the pulse scheme given in Figure 1 on an oriented bicelle sample. F_1-traces through the cross-peaks indicate that very good separation of the $^{13}C^{\alpha}$–$^{1}H^{\alpha}$ doublet components is achieved. In this regard it is noteworthy that the values of the one-bond $^{13}C^{\alpha}$–$^{1}H^{\alpha}$ dipolar coupling, D_{CH}, are −29.7, −0.8 and 19.9 Hz for Ala 28, Pro 19 and Phe 4, respectively, and that the range of couplings measured in this sample extends from −30 to 20 Hz (see below). Thus, the degree to which each of the doublet components are separated into individual data sets for all of the amino acids in the protein is well represented by the separation of components for the residues selected in Figure 2.

In order to establish the reproducibility of the method the experiment was repeated twice, with the results shown in Figure 3a. A good correlation between dipolar coupling values measured from the two experiments was obtained with a pairwise root-mean-squared-deviation (rmsd) of 1.35 Hz for the 63 residues considered. It is also possible to compare results from the present method with dipolar couplings that are obtained using different experiments. Figure 3b shows a comparison between the results obtained using the method of Figure 1 (referred to as method 1) with a similar frequency-based measurement approach in which couplings are obtained from splittings in the H^{α} proton dimension of an HA(CACO)NNH-based experiment (method 2) (Grzesiek and Bax, 1993). In this case a pairwise rmsd of 1.8 Hz is obtained.

The values of D_{CH} obtained from the scheme of Figure 1 are compared with predicted dipolar couplings established from the X-ray derived structure of ubiquitin (Vijay-Kumar et al., 1987) in Figure 3c. Calculated values were obtained using the relation (Tjandra and Bax, 1997a),

$$D_{PQ}(\theta,\phi) = -S(\mu_o/4\pi)\gamma_P\gamma_Q h \,/\, (4\pi^2 r_{PQ}^3) \\ [A_a(3\cos^2\theta - 1) + 3/2A_r\sin^2\theta\cos 2\phi] \qquad (2)$$

where γ_i is the gyromagnetic ratio of spin i, h is Planck's constant, r_{PQ} is the distance between spins P and Q, S is the order parameter describing the amplitude of PQ bond vector motion, A_a and A_r are the axial and rhombic components of the molecular

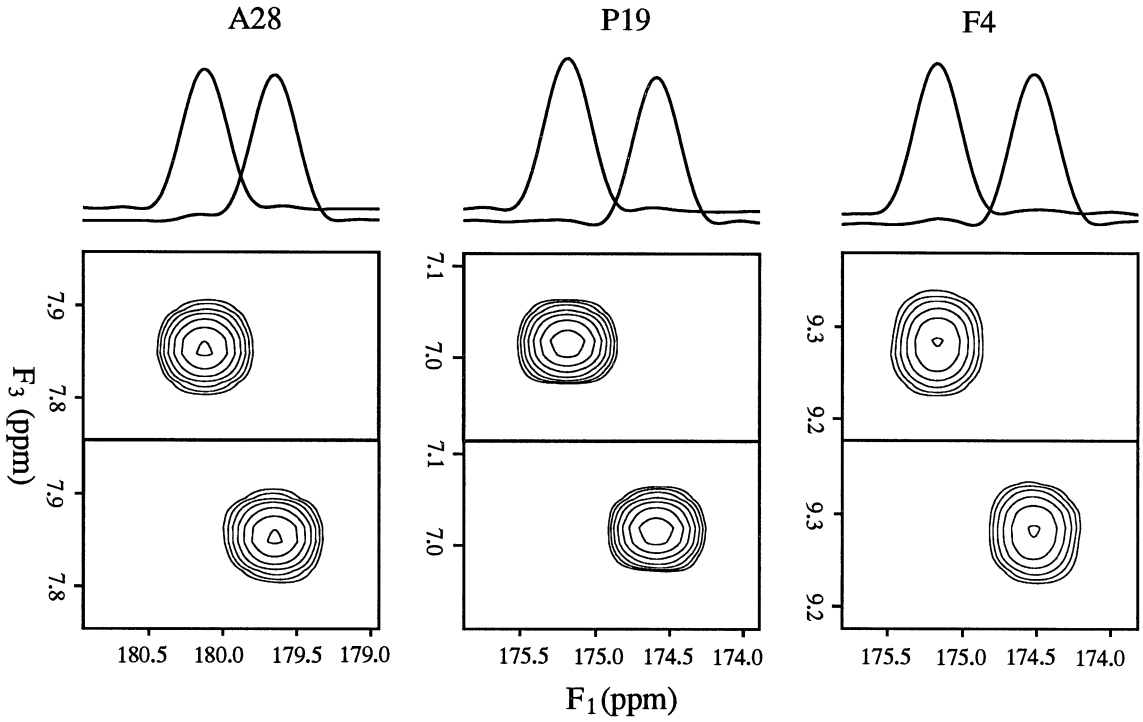

Figure 2. F_1 cross-sections through cross-peaks from Ala 28 ($D_{CH}=-29.7$ Hz), Pro 19 ($D_{CH}=-0.8$ Hz) and Phe 4 ($D_{CH}=19.9$ Hz) obtained from spectra recorded at 35 °C. Individual doublet components were separated into two spectra according to the method described in the text with software written in-house. Spectra were recorded using the scheme of Figure 1 in an interleaved manner, with 16 scans/FID giving rise to a total acquisition time of 22 h (for each temperature). Spectral widths in (F_1,F_2,F_3) of (1200 Hz, 1063.5 Hz, 7993.6 Hz) and net acquisition times of (23.3 ms, 18.8 ms, 64 ms) in (t_1,t_2,t_3) were employed. Each of the t_1 and t_2 time domains were apodized using cosine-bell window functions. The digital resolution was improved in F_1 by zero-filling the t_1 time domain to 512 points prior to Fourier transformation. The t_2 time domain data was doubled using mirror image linear prediction (Zhu and Bax, 1990), apodized and zero filled to 128 complex points. A 65° shifted sine-bell-squared window function was used in t_3 and the data zero-filled to 1 K points prior to transformation. All data sets were processed with NMRPipe (Delaglio et al., 1995) and analysis performed with PIPP/CAPP (Garrett et al., 1991).

alignment tensor of the molecule and θ,ϕ define the orientation of the *PQ* vector in the principle coordinate axis system of the molecular alignment tensor. The values of A_a, A_r and the Euler angles describing the orientation of the principle alignment axis system with respect to the axis system in which the X-ray structure coordinates are defined were obtained by a least squares minimization grid-search procedure using both ^{15}N–NH and $^{13}C^{\alpha}$–$^{1}H^{\alpha}$ dipolar coupling data as input. Note that the order parameter in Equation 2 derives from motions occurring on timescales ranging from 10^{-12} to 10^{-2} s. Currently the only values available for S are from molecular dynamics simulations or from NMR spin relaxation measurements, both of which are restricted to the measurement of dynamics on ps-ns timescales. Simulations on a 25 residue zinc finger peptide have shown that S^2 values for backbone $^{13}C^{\alpha}$–$^{1}H^{\alpha}$ pairs are on average higher by 0.06 units than S^2 values for ^{15}N-NH bond vectors (Palmer and Case, 1992). Values of S of 0.92 (Tjandra et al., 1995) and 0.95 for ^{15}N–NH and $^{13}C^{\alpha}$–$^{1}H^{\alpha}$ bond vectors were thus used in the present minimization and $(A_a,A_r) = (7.5\times10^{-4},1.5\times10^{-4})$ obtained. Essentially identical A_a and A_r values of $(7.5\times10^{-4},1.5\times10^{-4})$ and $(7.6\times10^{-4},1.7\times10^{-4})$ are obtained from separate fits using only the ^{15}N–NH or only $^{13}C^{\alpha}$–$^{1}H^{\alpha}$ dipolar data, respectively. The pairwise rmsd between predicted and measured values of D_{CH} is 2.9 Hz and this difference likely reflects small deviations between solution and crystal forms of the protein, errors in the crystal structure coordinates, departures from the simplistic assumption concerning the nature of the internal motions of the protein and a number of potential errors in the measurements themselves.

One possible source of error in measured D_{CH} values derives from cross-correlated spin relaxation occurring during the interval extending from *d* to *e* in

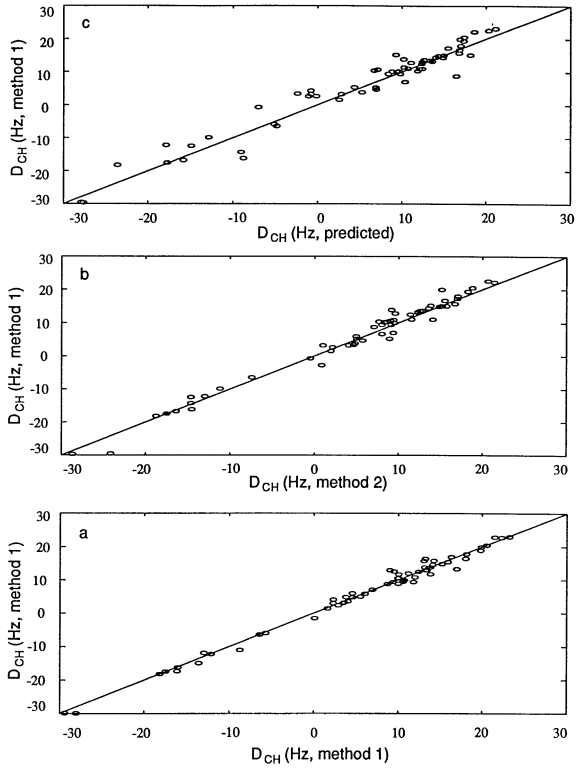

Figure 3. (a) Comparison of D_{CH} values measured from two sets of spectra recorded with the scheme of Figure 1 (method 1). A pairwise rmsd of 1.35 Hz is obtained. (b) Comparison of D_{CH} values obtained using method 1 with dipolar couplings from an alternative frequency domain approach (method 2) where $^{13}C^{\alpha}$–$^{1}H^{\alpha}$ couplings are measured from splittings in the proton dimension of an HA(CACO)NNH-based experiment (see text). Doublet components were separated into individual data sets using an identical procedure to that described in the text for the scheme of Figure 1. The pairwise rmsd between the two data sets is 1.8 Hz. (c) Predicted D_{CH} vs. measured D_{CH} values using method 1. The X-ray derived structure of ubiquitin (Vijay-Kumar et al., 1987) was used to calculate D_{CH}(predicted) as discussed in the text. A pairwise rmsd of 2.9 Hz is obtained.

Figure 1. The major source of relaxation interference is due to the $^{13}C^{\alpha}(j)$–$^{1}H^{\alpha}(j)$ dipolar interaction and a second dipolar effect involving the $^{13}C^{\alpha}$ spin and a proximal proton, ^{1}H(i), that is also coupled to $^{13}C^{\alpha}$. In this case each of the $^{13}C^{\alpha}(j)$ doublet components arising from the coupling with $^{1}H^{\alpha}(j)$ is further split by coupling of the $^{13}C^{\alpha}$ spin with $^{1}H(i)$. In macromolecular applications the $^{13}C^{\alpha}(j)$–$^{1}H(i)$ coupling will not be resolved and in the absence of the cross-correlation effect mentioned above the center of each of the components arising from the $^{13}C^{\alpha}$-$^{1}H^{\alpha}$ coupling does not change. In the case where cross-correlated relaxation is non-zero, however, each of the two (unresolved) lines produced by the $^{13}C^{\alpha}(j)$–$^{1}H(i)$ coupling will have different linewidths, perturbing the positions of the $^{13}C^{\alpha}$–$^{1}H^{\alpha}$ doublets, with the separation between the doublets decreasing (increasing) for positive (negative) cross-correlation relaxation rates (Tjandra and Bax, 1997b). Hence measured $J_{CH}+D_{CH}$ values will be in error. It is noteworthy that in the macromolecular limit the cross-correlation effect is proportional to the molecular tumbling time, as discussed in some detail by Tjandra and Bax. (1997b).

Two limiting cases regarding the coupling of $^{13}C^{\alpha}(j)$ and $^{1}H(i)$ must be considered with regards to the effects of cross-correlated spin relaxation on measured peak positions. In the case that the $^{13}C^{\alpha}(j)$-$^{1}H(i)$ splitting arises predominately from scalar coupling (the $^{13}C^{\alpha}$(j)–$^{1}H(i)$ bond vector is oriented near the magic angle with respect to the principle axis of an axially symmetric alignment tensor, for example) the cross-correlated relaxation induced errors in measured peak splittings will be approximately the same in experiments performed on oriented and unoriented samples. Hence, the extracted D_{CH} values are largely independent of this effect. Note that since the orientation of the sample is achieved by an increase in temperature relative to the unoriented state (10 °C in the present experiments) there will be a concomitant decrease in correlation time leading to an incomplete cancellation of errors from cross-correlation. In the case of the ubiquitin sample that we have used there is an increase in average correlation time by a factor of 1.17 for a temperature decrease from 35 to 25 °C.

In contrast to the case considered above, if the coupling between $^{13}C^{\alpha}(j)$ and $^{1}H(i)$ arises from dipolar as opposed to scalar effects, the splitting from the $^{13}C^{\alpha}(j)$–$^{1}H(i)$ interaction will only be present when the sample is oriented and errors from cross-correlation will not cancel when D_{CH} is calculated from the difference between splittings measured in oriented and unoriented samples. For the majority of $^{13}C^{\alpha}(j)$ spins the coupling with $^{1}H(i)$ will include contributions from both scalar and dipolar terms and it is important to establish the size of the errors in D_{CH} that might therefore be expected.

In the case of the pulse scheme of Figure 1 $^{13}C^{\alpha}$–$^{1}H^{\alpha}$ couplings are measured during a non-constant time evolution period which extends for a duration $\kappa t_{1,\max} \approx 12$ ms. Linewidths in the F_1 dimension of the Fourier transformed dataset are thus dominated by the effects of the limited acquisition time, the $^{13}C^{\alpha}$–$^{13}C^{\beta}$ one bond coupling, and the significant weighting function that must be applied to the time domain in order to minimize truncation artifacts.

This reduces the relative differences in linewidths of cross-peaks and hence errors which result from cross-correlation. Consider an AMX spin system where A=$^{13}C^{\alpha}$, M=$^{1}H^{\alpha}$, X=^{1}H with r_{AM}=1.1Å, r_{AX}=2.2Å, $J_{AM}+D_{AM}$=140 Hz, $J_{AX}+D_{AX}$=10 Hz. Note that r_{AX}=2.2Å approximates the distance of closest approach for C^{α}–H^{β} spins in proteins. From the equations provided in Tjandra and Bax (1997b) it is straightforward to show that in the macromolecular limit the ratio of the relaxation rates of the components arising from the *A–X* coupling differ by less than a factor of 1.3. Simulations with a $t_{1,\max}$ of 12 ms and employing the same time-domain weighting functions as used for the experimental data establish that the peak positions of each of the $^{13}C^{\alpha}$ *AM* doublet components are affected by less than 0.1 Hz from the *AX* coupling. It is noteworthy that a $J_{AX}+D_{AX}$ value of 10 Hz is approximately a factor of two larger than the largest *AX* coupling that would be predicted for the degree of alignment present in the sample considered in this study. Therefore, cross-correlated spin relaxation is unlikely to introduce significant errors in measured dipolar couplings using the sequence of Figure 1.

It is important to recognize, however, that the situation may be quite different in the case where $^{13}C^{\alpha}$–$^{1}H^{\alpha}$ couplings are recorded during a constant-time evolution period. For example, consider the constant-time scheme, $T + t_1/2$ 180(^{13}C) $T - t_1/2$, with $^{13}C^{\alpha}$ transverse magnetization present at the start. In this case F_1 linewidths of all multiplet components will be equivalent, but peak intensities will be modulated according to $\exp(-2R_iT)$, where R_i is the relaxation rate of multiplet component *i*. The relative ratios of components will thus be preserved in a manner independent of the length of acquisition, t_1, or the applied window function, and cross-correlated spin relaxation effects of the type discussed above can introduce errors in the measured coupling values. Finally, it is noteworthy that in the case where D_{CH} values are measured from $^{1}H^{\alpha}$ frequency domain splittings errors in couplings may arise from interference effects between $^{13}C^{\alpha}(j)$–$^{1}H^{\alpha}(j)$,$^{1}H^{\alpha}(j)$–$^{1}H(i)$ dipolar interactions if there is a non-zero dipolar coupling between $^{1}H^{\alpha}$ and $^{1}H(i)$. In this case the cross-correlation effect can be considerably larger than for the $^{13}C^{\alpha}(j)$–$^{1}H^{\alpha}(j)$, $^{13}C^{\alpha}(j)$-$^{1}H(i)$ interaction. The size of the error will be a function of the acquisition time in the dimension in which the splitting is measured ($^{1}H^{\alpha}$), the weighting function used, the size of the $^{1}H^{\alpha}(j)$-$^{1}H(i)$ coupling and the ratio of the cross-correlation and auto-correlation relaxation terms of the individual multiplet components. Simulations show that errors on the order of 0.5–1 Hz can occur. The increase in the pairwise rmsd between D_{CH} values obtained using methods 1 and 2 (see above and Figure 3a,b) relative to the rmsd obtained from duplicate data sets recorded with the sequence of Figure 1 may well reflect in part the increased errors associated with ^{1}H frequency domain splitting measurements relative to ^{13}C-based experiments. We therefore prefer experiments where couplings are obtained from splittings in the carbon dimension.

A potential source of error in the present scheme derives from proton pulse imperfections. The ^{1}H 180° pulse which separates the two $\kappa t_1/2$ periods during which time the $^{13}C^{\alpha}$–$^{1}H^{\alpha}$ coupling evolves is particularly critical, since any non−180° character of this pulse leads to a reduction in the measured coupling. Simulations indicate that a 10% error in flip angle for a 180° pulse decreases the measured dipolar coupling by 0.25 Hz/κ or 0.5 Hz in our case. Experiments performed on our spectrometer indicate that for a composite inversion pulse errors in flip angle are under 7% and a comparison of the predicted and measured dipolar data does not suggest any systematic underestimate of the experimental couplings which might be expected from imperfections in this proton pulse.

In summary, we have described an HNCO-based sequence for the measurement of one-bond $^{13}C^{\alpha}$–$^{1}H^{\alpha}$ dipolar couplings in ^{15}N, ^{13}C labeled proteins. Values of D_{CH} are obtained from splittings of $^{13}C^{\alpha}$–$^{1}H^{\alpha}$ doublet components that are recorded in separate data sets, and in this manner spectral resolution is not compromised. The use of dipolar couplings in solution structure determination is a powerful supplement to existing methodology relying on restraints obtained from NOEs and scalar coupling constants.

Acknowledgements

The authors are grateful to Professor J. Wand (SUNY, Buffalo) for providing the sample of ubiquitin used in this study, to Dr J. Prestegard (University of Georgia) for sharing with us his method for improving bicelle stability and to Dr Dan Garrett (NIH) for assistance with the peak-picking routines in PIPP. This research was supported by a grant from the Medical Research Council of Canada. L.E.K is an International Howard Hughes Research Scholar. J.R. Tolman and N. K. Goto are the recipients of a Human Frontiers Post-doctoral Fellowship and an NSERC postgraduate scholarship, respectively.

References

Bax, A., and Ikura, M. (1991) *J. Biomol. NMR*, **1**, 99–104.

Bodenhausen, G., and Ernst, R. R. (1981) *J. Magn. Reson.*, **45**, 367–373.

Boyd, J., and Scoffe, N. (1989) *J. Magn. Reson.*, **85**, 406–413.

Delaglio, F., Grzesiek, S., Vuister, G. W., Zhu, G., Pfeifer, J., and Bax, A. (1995) *J. Biomol. NMR*, **6**, 277–293.

Freeman, R., Kempsell, S. P., and Levitt, M. H. (1980) *J. Magn. Reson.*, **38**, 453–479.

Garrett, D. S., Powers, R., Gronenborn, A. M., and Clore, G. M. (1991) *J. Magn. Reson.*, **95**, 214–220.

Grzesiek, S., and Bax, A. (1993) *J. Biomol. NMR*, **3**, 185–204.

Kay, L. E. (1993) *J. Am. Chem. Soc.*, **115**, 2055–2056.

Kay, L. E., Ikura, M., Tschudin, R., and Bax, A. (1990) *J. Magn. Reson.*, **89**, 496–514.

Kay, L. E., Keifer, P., and Saarinen, T. (1992) *J. Am. Chem. Soc.*, **114**, 10663–10665.

Logan, T. M., Olejniczak, E. T., Xu, R. X., and Fesik, S. W. (1993) *J. Biomol. NMR*, **3**, 225–231.

Marion, D., Ikura, M., Tschudin, R., and Bax, A. (1989) *J. Magn. Reson.*, **85**, 393–399.

McCoy, M., and Mueller, L. (1992) *J. Am. Chem. Soc.*, **114**, 2108–2110.

Muhandiram, D. R., and Kay, L. E. (1994) *J. Magn. Reson. Ser. B.*, **103**, 203–216.

Palmer, A. G., and Case, D. A. (1992) *J. Am. Chem. Soc.*, **114**, 9059–9067.

Patt, S. L. (1992) *J. Magn. Reson.*, **96**, 94–102.

Sanders, C. R., Hare, B. J., Howard, K. P., and Prestegard, J. H. (1994) *Prog. NMR. Spectrosc.*, **26**, 421–444.

Sanders, C. R., and Schwonek, J. P. (1992) *Biochemistry*, **31**, 8898–8905.

Schleucher, J., Sattler, M., and Griesinger, C. (1993) *Angew. Chem. Int. Ed. Engl.*, **32**, 1489–1491.

Shaka, A. J., Keeler, J., Frenkiel, T., and Freeman, R. (1983) *J. Magn. Reson.*, **52**, 335–338.

Sorensen, M. D., Meissner, A., and Sorensen, O. W. (1997) *J. Biomol. NMR*, **10**, 181–186.

Tjandra, N., and Bax, A. (1997a) *Science*, **278**, 1111–1114.

Tjandra, N., and Bax, A. (1997b) *J. Magn. Reson.*, **124**, 512–515.

Tjandra, N., Feller, S. E., Pastor, R. W., and Bax, A. (1995) *J. Am. Chem. Soc.*, **117**, 12562–12566.

Tjandra, N., Grzesiek, S., and Bax, A. (1996) *J. Am. Chem. Soc.*, **118**, 6264–6272.

Tjandra, N., Omichinski, J. G., Gronenborn, A. M., Clore, G. M., and Bax, A. (1997) *Nat. Struct. Biol.*, **4**, 732–738.

Tolman, J. R., Flanagan, J. M., Kennedy, M. A., and Prestegard, J. H. (1995) *Proc. Natl. Acad. Sci.*, **92**, 9279–9283.

Tolman, J. R., Flanagan, J. M., Kennedy, M. A., and Prestegard, J. H. (1997) *Nature Structure Biology*, **4**, 292–297.

Tolman, J. R., and Prestegard, J. H. (1996a) *J. Magn. Reson. Ser. B.*, **112**, 269–274.

Tolman, J. R., and Prestegard, J. H. (1996b) *J. Magn. Reson. Ser. B.*, **112**, 245–252.

Vijay-Kumar, S., Bugg, C. E., and Cook, W. J. (1987) *J. Mol. Biol.*, **194**, 531–544.

Vuister, G. W., and Bax, A. (1992) *J. Magn. Reson.*, **98**, 428–435.

Vuister, G. W., Delaglio, F., and Bax, A. (1992) *J. Am. Chem. Soc.*, **114**, 9674–9675.

Wüthrich, K. (1986) *NMR of Proteins and Nucleic Acids*, John Wiley and Sons, New York.

Yamazaki, T., Lee, W., Arrowsmith, C. H., Muhandiram, D. R., and Kay, L. E. (1994) *J. Am. Chem. Soc.*, **116**, 11655–11666.

Yang, D., and Nagayama, K. (1996) *J. Magn. Reson. Ser. A*, **118**, 117–121.

Zhu, G., and Bax, A. (1990) *J. Magn. Reson.*, **90**, 405–410.